*J Neuropathol Exp Neurol*
Vol. 75, No. 1, January 2016, pp. 19–34
doi: 10.1093/jnen/nlv001

ORIGINAL ARTICLE

# Characterization of Early Pathological Tau Conformations and Phosphorylation in Chronic Traumatic Encephalopathy

Nicholas M. Kanaan, PhD, Kristine Cox, DVM, Victor E. Alvarez, MD, Thor D. Stein, MD, PhD, Sharra Poncil, BS, and Ann C. McKee, MD

**Abstract**

Chronic traumatic encephalopathy (CTE) is a neurodegenerative tauopathy that develops after repetitive head injury. Several lines of evidence in other tauopathies suggest that tau oligomer formation induces neurotoxicity and that tau oligomer-mediated neurotoxicity involves induction of axonal dysfunction through exposure of an N-terminal motif in tau, the phosphatase-activating domain (PAD). Additionally, phosphorylation at serine 422 in tau occurs early and correlates with cognitive decline in patients with Alzheimer disease (AD). We performed immunohistochemistry and immunofluorescence on fixed brain sections and biochemical analysis of fresh brain extracts to characterize the presence of PAD-exposed tau (TNT1 antibody), tau oligomers (TOC1 antibody), tau phosphorylated at S422 (pS422 antibody), and tau truncated at D421 (TauC3 antibody) in the brains of 9-11 cases with CTE and cases of nondemented aged controls and AD (Braak VI) (n = 6, each). All 3 early tau markers (ie, TNT1, TOC1, and pS422) were present in CTE and displayed extensive colocalization in perivascular tau lesions that are considered diagnostic for CTE. Notably, the TauC3 epitope, which is abundant in AD, was relatively sparse in CTE. Together, these results provide the first description of PAD exposure, TOC1 reactive oligomers, phosphorylation of S422, and TauC3 truncation in the tau pathology of CTE.

**Key Words:** Alzheimer disease, Chronic traumatic encephalopathy, Dementia, Oligomers, Phosphatase-activating domain, Tauopathy, Traumatic brain injury.

From the Department of Translational Science and Molecular Medicine, College of Human Medicine, Michigan State University, Grand Rapids, Michigan (NMK, KC, SP); Hauenstein Neuroscience Center, Mercy Health Saint Mary's, Grand Rapids, Michigan (NMK); VA Boston Healthcare System, Boston, Massachusetts (VEA, TDS, ACM); Boston University Alzheimer's Disease Center, CTE Program, Boston University School of Medicine, Boston, Massachusetts (VEA, TDS, ACM); Department of Veterans Affairs Medical Center, Bedford, Massachusetts (TDS); Department of Pathology and Laboratory Medicine, Boston University School of Medicine, Boston, Massachusetts (TDS, ACM).

Send correspondence to: Nicholas M. Kanaan, PhD, Department of Translational Science and Molecular Medicine, College of Human Medicine, Michigan State University, 333 Bostwick Ave NE, Grand Rapids, MI 49503; E-mail: Nicholas.kanaan@hc.msu.edu

This work was supported by NIH grants R01 AG044372 and R01 NS082730 (NMK), the BrightFocus Foundation (A2013364S, NMK), the Department of Veterans Affairs (ACM); National Institute of Neurological Diseases and Stroke 1U01NS086659-01 (ACM), National Institute of Aging Boston University Alzheimer's Disease Center [P30AG13846; supplement 0572063345-5, ACM]; National Institute of Aging Boston University Framingham Heart Study R01 [AG1649, ACM]; Alzheimer's Association (NIRG-305779, TDS); Sports Legacy Institute (ACM); National Operating Committee on Standards for Athletic Equipment (ACM); the Veterans Affairs Biorepository (CSP 501, ACM); Translational Research Center for Traumatic Brain Injury and Stress Disorders (TRACTS) Veterans Affairs Rehabilitation Research and Development Traumatic Brain Injury Center of Excellence (B6796-C, ACM), unrestricted gifts from the National Football League, the Andlinger Foundation and the World Wrestling Entertainment, Inc. (WWE) (ACM), the Brain and Body Donation Program is supported by the National Institute of Neurological Disorders and Stroke (U24 NS072026 National Brain and Tissue Resource for Parkinson's Disease and Related Disorders), the National Institute on Aging (P30 AG19610 Arizona Alzheimer's Disease Core Center), the Arizona Department of Health Services (contract 211002, Arizona Alzheimer's Research Center), the Arizona Biomedical Research Commission (contracts 4001, 0011, 05-901, and 1001 to the Arizona Parkinson's Disease Consortium), the Michael J. Fox Foundation for Parkinson's Research, and the Alzheimer's Disease Core Center grant (P30 AG013854) from the National Institute on Aging to Northwestern University, Chicago Illinois.

The authors have no duality or conflicts of interest to declare.

Supplementary Data can be found at http://www.jnen.oxfordjournals.org.

## INTRODUCTION

Chronic traumatic encephalopathy (CTE) is a progressive neurodegenerative disease that is found in individuals with a history of repetitive mild brain trauma (eg, athletes and military personnel) (1–3). Although recognition of the clinical symptoms of CTE was first reported by Martland in 1928 (4), the first large clinicopathological series of CTE was published in 1973 by Corsellis and colleagues, who described neurofibrillary degeneration of the substantia nigra and cerebral cortex using Von Braunmühl silver stain (5). The distinctive perivascular pattern of abnormally phosphorylated tau pathology in CTE was first observed by Geddes et al in 1999, who also noted the preferential distribution at the depths of the cerebral sulci (6). In 2013, McKee and coworkers reported the clinical and immunohistochemical characteristics of 68 subjects with CTE and introduced pathological criteria for the neuropathological diagnosis of CTE (7).

The current criteria for the pathological diagnosis of CTE are based on hallmark features that include perivascular accumulation of phosphorylated tau in a strikingly irregular pattern concentrated at the depths of cerebral sulci (7); [http://

www.ninds.nih.gov/research/tbi/ReportFirstNIHConsensusConference.htm]. Pathological tau inclusions in CTE are found in neurons as pretangles and neurofibrillary tangles (NFTs), in astrocytes as thorn-shaped astrocytes, and in dot-like and thread-like cellular processes around small blood vessels, and in the neuropil (3). Other pathological features of CTE include axonal loss, neuroinflammation, accumulation of phosphorylated deposits of TDP-43, and substantial brain atrophy. A four-stage staging system was recently described to identify the severity of pathological tau deposition in CTE (7). In stage I of CTE, isolated focal perivascular tau lesions are found at sulcal depths of the cortex. In stage II, perivascular tau lesions are found in multiple sites in multiple cortical regions, and there is mild involvement of subcortical regions (eg, locus coeruleus and substantia nigra). Progression into stage III CTE is characterized by more widespread cortical pathology and involvement of medial temporal lobe structures (ie, hippocampus, amygdala, and entorhinal cortex) and additional subcortical regions. Finally, in stage IV CTE, there is cerebral atrophy and neuronal loss that is accompanied by widely distributed tau pathology throughout the cortex, medial temporal lobe, diencephalon, and brainstem.

Previous studies used traditional markers of disease-related tau phosphoepitopes such as PHF1, CP13, and AT8 antibodies to label the tau inclusions (6–10), and there are reports of biochemical analyses of tau isolated from CTE brains (11, 12). Together, these existing studies have not investigated the progressive evolution of pathological changes in tau protein that are associated with CTE. By contrast, in Alzheimer disease (AD), we know that tau pathology undergoes a stereotypical sequence of changes (eg, phosphorylation, conformational shifts, and truncation) that are identified using various tau antibodies as the pathology progresses (13, 14). For example, phosphorylation of serine 422 (identified using the pS422 antibody) occurs in early, pretangle neurons, and progressive accumulation of pS422 tau pathology in the cholinergic basal forebrain correlates well with cognitive decline across nondemented aged control (ND), mild cognitively impaired (MCI), and AD cases (15–17). Following some conformational and phosphorylation changes (eg, the Alz50 conformation, pS422, AT8, and pT231) and as the pathological inclusions mature from the early stages through the later stages, the C-terminus is cleaved at aspartic acid 421, giving rise to the neoepitope of the TauC3 antibody in AD (13–22). In addition, 2 recently identified pretangle stage changes in tau appear to confer toxicity to the tau protein (23–26). Tau contains a biologically active motif in the amino terminus of tau, called the phosphatase-activating domain ([PAD], amino acids 2–18), and aberrant exposure of PAD triggers a signaling cascade that impairs fast anterograde axonal transport (24, 27). The TNT1 antibody is a marker that indicates whether PAD is exposed in tau, and the pattern of TNT1 staining in neurons suggests PAD exposure is a very early pretangle pathological change in tau in AD (23, 24). Second, a recently characterized antibody called tau-oligomer complex 1 (TOC1) selectively labels tau oligomers over monomeric or filamentous tau (25, 26, 28–30). A number of disease-relevant modifications of tau, including oligomer formation, appear to alter tau conformation in ways that aberrantly expose PAD (29, 31). Thus, both TNT1 and TOC1 are pretangle pathological tau changes in AD that may indicate potential toxic mechanisms of tau pathologies, and pS422 is an early change that is well correlated with cognitive decline. The hypothesis that the earliest modifications in tau drive its toxicity is consistent with accumulating evidence that the classical inclusions (such as NFTs) are not the toxic form of tau (32, 33), but rather it is the small, misfolded oligomeric species (29, 34–37).

In the current work, we sought to identify whether pathological changes in tau, such as PAD exposure, oligomer formation, phosphorylation at S422, and C-terminal truncation are also characteristic of CTE pathology. These 4 markers are particularly useful in understanding potential posttraumatic events in CTE because PAD exposure impairs axonal transport (24), oligomers confer toxicity (28, 38–40), pS422 correlates with cognitive decline (15), and D421 truncated tau may be related to cell toxicity (41, 42). Using a combination of immunohistochemical and biochemical analyses, we provide the first description of PAD exposure, tau oligomers, S422 phosphorylation, and C-terminal cleaved tau in CTE and characterize the types of pathological lesions composed of these abnormal tau forms. In CTE, neuronal and glial tau pathologies contained PAD-exposed tau (TNT1-reactive), tau oligomers (TOC1-reactive), and phosphorylated S422 tau (ps422-reactive), and all 3 forms of pathology were highly colocalized. While the types of neuronal and glial pathologies in CTE share some features with AD, other tauopathies, and normal aging, there are several important distinctions (2, 43). For example, the TauC3 epitope that is abundant in AD was very infrequent in CTE, and dot-like neurites, a common feature in CTE, are infrequent in AD. Furthermore, biochemical and immunohistological analyses of TNT1, TOC1, and pS422 tau all showed high levels in CTE brain samples, in contrast to the very low levels in ND. Collectively, these data suggest some of the early phosphoepitopes and conformational tau changes that are linked to potential mechanisms of toxicity in AD also occur in CTE, although with some notable distinctions.

## MATERIALS AND METHODS

### Human Subjects

For the immunohistochemical analyses, 9 cases of CTE without comorbid pathology including the absence of β-amyloid plaques (CTE stage II, n = 2; CTE stage III, n = 5; and CTE stage IV, n = 2) were obtained from the Boston University Alzheimer's Disease Center (BU ADC) CTE Program and VA Boston (Boston, MA). Fixed tissue sections from temporal cortex of 6 ND and 6 severe AD cases (Braak VI) were obtained from the Alzheimer's Disease Research Center at Banner Sun Health Research Institute (Sun City, AZ) (44). Fresh frozen brain tissue samples from 23 cases were used for the biochemical analyses consisting of 11 cases of CTE (CTE stage II/III, n = 5; CTE stage IV, n = 6), obtained from the BU ADC CTE Program, as well as 6 ND (Braak II) and 6 cases of AD (Braak VI) obtained from the Brain Bank of the Cognitive Neurology and Alzheimer's Disease Center at Northwestern University (Chicago, IL).

All CTE cases met pathological criteria for the diagnosis of CTE (3) and were staged according to severity and distribution of tau pathology using an antibody to phosphorylated PHF-tau (AT8; Pierce Endogen, Rockford IL; 1:2,000), as described (43). All cases of CTE were free of comorbid neurodegenerative disease or other neuropathologies. Neuropathologists (ACM, TDS) performed the neuropathological evaluation blinded to all patient medical history, clinical symptoms, and APOE genotype. For detailed human subject information, see Supplementary Data 1 (a table containing data on the cases used in this study).

## Tau Purification From Fresh Frozen Frontal Cortex Samples

Soluble and sarkosyl-insoluble tau fractions were prepared from flash frozen frontal cortex tissue of ND, CTE, and AD cases. Each extraction was prepared by homogenizing 0.5 to 1 gram of frontal cortex on ice in 10 volumes (1 g = 10 mL) of brain homogenization buffer (50 mM Tris pH 7.4, 274 mM NaCl, 5 mM KCl, 1 mM phenylmethylsulfonyl fluoride, and 10 µg/mL each of pepstatin, leupeptin, bestatin, and aprotinin). The soluble tau fraction was collected in the supernatant following centrifugation at 27,000 x *g* for 20 minutes at 4°C. The remaining pellet was homogenized further in brain pellet homogenization buffer (10 mM Tris pH 7.4, 800 mM NaCl, 10% sucrose, 1 mM ethylene glycol-bis(2-aminoethylether)-*N*,*N*,*N*′,*N*′-tetraacetic acid, 1 mM phenylmethylsulfonyl fluoride), and centrifuged as above. The supernatants were collected, sarkosyl was added to a final concentration of 1%, incubated at 37°C for 1 hour, and then centrifuged at 200,000 x *g* for 1 hour at 4°C. Lastly, the final pellet was resuspended in 1 mL of brain pellet homogenization buffer representing the sarkosyl insoluble tau fraction. Both the soluble tau and sarkosyl insoluble tau fractions were assayed for total protein concentration using the Lowry protein assay and stored at −80°C until used in sandwich enzyme-linked immunosorbent assays (ELISAs).

## Primary Antibodies

A number of tau antibodies were used that are characterized in AD but not in CTE (Table 1). The TNT1 antibody (mouse IgG1, Binder/Kanaan Lab, Michigan State University, Grand Rapids, MI) was made against PAD (ie, amino acids 2–18), and TNT1 is a marker of pathological conformations in which PAD is exposed in tissue sections and nondenaturing assays (23, 24). The TOC1 antibody (mouse IgM, Binder/Kanaan Lab) has an epitope between 209–224 (numbering based on full-length tau containing 441 amino acids) and selectively recognizes oligomeric tau aggregate conformations, compared to monomeric tau or filamentous aggregate conformations (25, 26). The pS422 antibody is a monoclonal rabbit antibody (79415, Abcam, Cambridge, MA) that recognizes tau when serine 422 is phosphorylated. In the cholinergic basal forebrain, the accumulation of pS422 tau pathology is well correlated with cognitive decline during the progression of AD (15). All 3 antibodies used here (ie, pS422, TNT1, and TOC1) are markers of early, pretangle tau pathology in AD and other tauopathies (15–17, 23–26). TauC3 is an antibody (mouse IgG1, Binder/Kanaan Lab) that recognizes tau truncated at D421 (22), a modification that appears later in the early phases of NFT development and increases with progression in AD (13–16, 18–21). Astrocytes were identified using a glial fibrillary acidic protein antibody ([GFAP], mouse IgG1, G3893, Sigma, St. Louis, MO), and microglia were identified using a human leukocyte antigen–DR antibody ([HLA-DR], clone LN3, mouse IgG2b, 8693031, MP Biomed, Santa Ana, CA). The R1 antibody (Binder Lab), a rabbit polyclonal pan-tau antibody with numerous epitopes throughout the tau protein (45), was used in the sandwich ELISAs. The Tau5 antibody (mouse IgG1, Binder/Kanaan Lab) is a mouse monoclonal antibody with an epitope between 210–230 (46), which is unaffected by phosphorylation or conformation; this antibody was used in the sandwich ELISAs (Table 1).

## ELISA

Novel sandwich ELISAs were developed to measure the relative quantities of each form of tau present in the soluble and sarkosyl-insoluble tau fractions in the frontal cortex from ND, CTE, and AD brains. The levels of total tau, PAD-exposed tau, oligomeric tau, or C-terminal truncated tau were measured using the mouse monoclonal Tau5, TNT1, TOC1, or TauC3 antibody as the capture antibody, respectively. The R1

**TABLE 1.** Primary Antibodies

| Antibody | Epitope | Host | Isotype | IHC | IF | ELISA | Source |
|---|---|---|---|---|---|---|---|
| pS422 | Phospho S422 | Rb | IgG | 1:2500 | 1:1000 | 1:500 (cap) | 79415 (Abcam, Cambridge, MA) |
| TNT1 (PAD exposed tau) | aa 2–18 | Ms | IgG1 | 1:400000 | 1:30000 | 1:500 (cap) | Binder/Kanaan |
| TOC1 (oligomeric tau) | aa 209–224 | Ms | IgM | 1:5000 | 1:2000 | 1:500 (cap) | Binder/Kanaan |
| TauC3 | cleaved at D421 | Ms | IgG1 | 1:10000 | – | 1:500 (cap) | Binder/Kanaan |
| R1 | Pan-tau (multiple) | Rb | IgG | – | – | 1:10000 (det) | Binder |
| Tau5 | Pan-tau (aa 210–230) | Ms | IgG1 | – | – | 1:1000 (cap)1:40000 (det) | Binder/Kanaan |
| GFAP | Astrocytes | Ms | IgG1 | – | 1:400 | – | G3893 (Sigma, St. Louis, MO) |
| HLA-DR | Microglia | Ms | IgG2b | – | 1:100 | – | 8693031 (MB Biomed, Santa Ana, CA) |

Note: All Binder/Kanaan primary antibodies are diluted from a 1-mg/mL stock solution. cap, capture antibody for sandwich ELISAs; det, detection antibody for sandwich ELISAs; HLA-DR, human leukocyte antigen–DR; GFAP, glial fibrillary acidic protein; IF, immunofluorescence; IHC, immunohistochemistry; Ms, mouse; Rb, rabbit; TOC1, tau-oligomer complex 1; PAD, phosphatase-activating domain (PAD).

tau antibody (a polyclonal rabbit pan-tau antibody unaffected by phosphorylation) was used for detection of bound tau. The levels of tau phosphorylated at S422 were measured using the rabbit pS422 antibody as the capture antibody and the mouse monoclonal Tau5 antibody (a pan-tau antibody unaffected by phosphorylation) for the detection of bound tau. All steps were performed at room temperature; 200 μL/well were used for the rinsing and blocking steps; and 50 μL/well were used for all other steps. Capture antibodies were diluted (Tau5 at 1 μg/mL; TNT1, TOC1 pS422, or TauC3 at 2 μg/mL) in borate saline (100 mM boric acid, 25 mM sodium tetraborate decahydrate, 75 mM NaCl, 250 μM thimerosal) and incubated in high binding ELISA microplates (Corning, #3590, Thermo Fisher Scientific, Waltham, MA) for 1 hour. Plates were rinsed twice with ELISA wash buffer (100 mM boric acid, 25 mM sodium tetraborate decahydrate, 75 mM NaCl, 250 μM thimerosal, 0.4% bovine serum albumin, and 0.1% tween-20) and blocked with ELISA wash containing 5% nonfat dried milk for 1 hour. Each well was rinsed 2 times, and then the samples were added to the well for 1.5 hours. Human brain extracts were diluted to a final total protein concentration of 0.4 μg/μL (ie, 20 μg/well) for soluble tau fractions or 0.08 μg/μlL (ie, 4 μg/well) for insoluble tau fractions, and 50 μL/well was used in each ELISA. The optimal protein amounts for each fraction were determined in titering experiments to ensure the ELISAs were performed within the linear rage of reactivity. Wells were rinsed twice, and then R1 (0.1 μg/mL) or Tau5 (0.025 μg/mL) detection antibodies were diluted in blocking reagent, and added to each well for 1.5 hours. Wells were rinsed 3 times and incubated for 1.5 hours with goat anti-rabbit antibody conjugated to horseradish peroxidase (PI-1000, Vector Laboratories, Burlingame, CA) or horse anti-mouse conjugated to horseradish peroxidase (PI-2000, Vector Laboratories) diluted (0.2 μg/mL) in blocking reagent. The wells were rinsed 3 times, signal was detected by developing with TMB (3,3',5,5'-tetramethylbenzidine, Sigma) for 12 minutes, and then the reaction was stopped using 3.5% sulfuric acid. Tau standard ELISAs were performed with the human sample sandwich ELISAs to estimate the amount of tau captured by Tau 5, TNT1, TOC1, pS422, or TauC3. For the tau standards, a serial dilution of recombinant full-length human tau protein (produced as described previously [46]) ranging from 200 to 0.2 ng was bound to the ELISA plate for 1 hour, then blocked as above; detection was performed using either R1 or Tau5 antibodies and HRP-secondary antibodies exactly as in the sandwich ELISAs. Each standard was run in duplicate and developed simultaneously with the sandwich ELISAs to ensure accurate interpolation of unknown tau amounts. The standard curve data were $\log_{10}$ transformed and best fit to a sigmoidal curve ($r^2 = 0.996$ for both). This provided a standard curve of absorbance values that were derived from R1 or Tau5 reactivity with known amounts of tau protein. The quantity of tau (ng) in each human sample was interpolated from the tau standard curves and then converted to a concentration of ng/μL by dividing the interpolated quantity by the volume of the sample used (ie, 50 μL). Supplementary Data 2 illustrates and provides an example of the tau standard and sandwich ELISAs used here. In all assays, wells with the samples omitted were used as blanks to obtain background levels that were subtracted from sample signals.

## Immunohistochemistry

Fixed tissue sections (cut at 50 μm) from the superior frontal gyrus (CTE) were processed for immunohistochemistry (IHC) using pS422, TNT1, TOC1, and TauC3 antibodies. Forty-μm-thick sections from the temporal lobe of ND and AD cases were included as references for the pathological tau lesions. For detailed information regarding the tissue fixation and processing protocols from each tissue resource see Supplementary Data 3 (a description of the fixation and tissue processing procedures at BU and Banner Sun Health). The blocking, peroxidase quenching, avidin-biotin complex labeling, and all rinsing steps were performed as previously described (47). Primary antibodies (Table 1) were incubated with the tissue sections overnight at 4°C, followed by a 2-hour incubation in biotinylated goat anti-mouse IgG (heavy plus light chains) secondary antibody (BA-9200, diluted 1:500) for TNT1 and TauC3, biotinylated goat anti-mouse IgM secondary antibody (BA-2020, diluted 1:500) for TOC1, or biotinylated goat anti-rabbit IgG (H+L) secondary antibody (BA-1000, diluted 1:500) for pS422 (all from Vector Laboratories). The labeling was developed with 3,3′-diaminobenzidine (Sigma, D5637), which produces a brown chromogen. Following IHC development, the sections were mounted and processed for Nissl counterstaining using the Cresyl violet protocol previously described (48). Control sections with the primary antibody omitted were performed to ensure the IHC signals were derived from tau antibody labeling and not due to nonspecific reactivity with the tissue (Supplementary Data 4, photomicrographs of primary delete control sections). Staining penetration through the entire z-axis of the tissue sections was confirmed by focusing through the sections at high magnification (ie, 60x/1.4 na). Image z-stacks (0.5-μm step size) were acquired with a Nikon Eclipse 90i microscope, a Nikon DS-Ri1 camera, and Nikon Elements AR software (Nikon Instruments Inc., Melville, NY), and the images (displayed using the extended depth of focus function) were prepared for publication using Adobe Photoshop and Illustrator.

## Triple-Label Immunofluorescence for Confocal Microscopy

Triple-label immunofluorescence (IF) was used to characterize the colocalization between either tau phosphorylated at S422, tau with PAD-exposed and tau oligomers, or between pS422 tau and glial cell markers. Tissue sections (same as above) from CTE and AD cases were processed for triple-label IF using the TNT1, TOC1, and pS422 antibodies. Glial cells were identified using anti-GFAP or anti-HLA-DR antibodies, and tau inclusions were labeled with pS422. All staining for IF was done according to published methods (48, 49). For the colocalization of TNT1, TOC1, and pS422, the sections were incubated overnight at 4°C in a primary antibody solution containing each antibody followed by incubation in a secondary antibody solution of Alexa Fluor 488 goat anti-mouse IgG1-specific (A-21121), Alexa Fluor 568 goat anti-mouse IgM-specific (A-21043), and Alexa Fluor 405 goat anti-rabbit specific (A-31556) antibodies (all from Invitrogen, Billerica, MA, diluted 1:500) for 2 hours. For the colocalization of pS422, GFAP, and HLA-DR, the sections were incubated overnight at

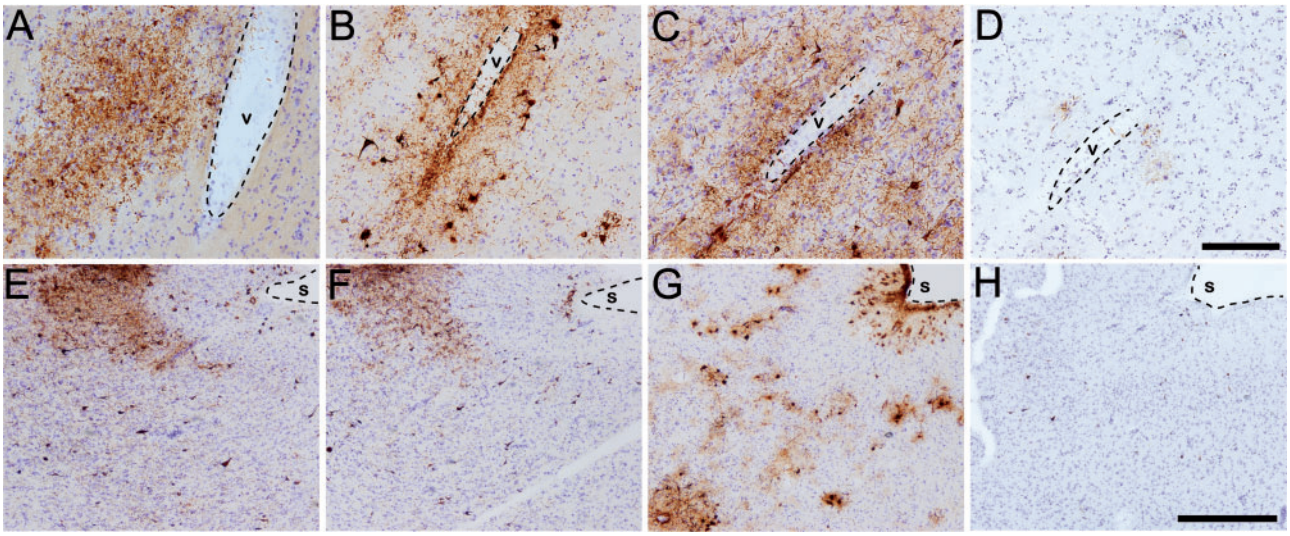


**FIGURE 1.** Antibodies to TNT1, TOC1, and pS422 label tau pathology in chronic traumatic encephalopathy (CTE). **(A–D)** Perivascular (v-vessel, dashed outline) tau pathology is immunoreactive for TNT1 **(A)**, TOC1 **(B)**, and pS422 **(C)**. Note the sparse presence of TauC3 **(D)** pathology in CTE. **(E–H)** Tau pathology in CTE is often patchy and most severe at the depths of the cortical sulci (s, dashed outline) and labeled with all 3 early pathology antibodies: TNT1 **(E)**, TOC1**(F)**, and pS422 **(G)**. Again, note the infrequent nature of TauC3 **(H)** reactive pathology in CTE. Scale bar in **D**, 200 μm for **A–D**; scale bar in **H**, 500 μm for **E–H**.

4°C in a primary antibody solution containing each antibody followed by incubation in a secondary antibody solution of Alexa Fluor 647 goat anti-rabbit specific (A-21244), Alexa Fluor 568 goat anti-mouse IgG1-specific (A-21124), and Alexa Fluor 488 goat anti-mouse IgG2b-specific (A-21141), antibodies (diluted 1:500) for 2 hours. Following the staining procedure, sections were mounted on microscope slides; autofluorescence was blocked using Sudan black (BP109-10; Thermo Fisher Scientific), as described (23, 24, 47), and then coverslipped using Vectashield hardset mountant (H-1400; Vector Labs, Burlingame, CA). Control sections where one of the primary antibodies was omitted confirmed that each secondary label was specific to the appropriate primary antibody because no staining was observed with the fluorophore for the omitted antibody (Supplementary Data 5, confocal photomicrographs of IF control sections). Image z-stacks (0.5 μm step size) were taken using a Nikon A1+ laser scanning confocal microscope system equipped with 488, 561, and 640 solid-state lasers, Nikon Elements AR software, and the images (maximum intensity projections) were prepared for publication using Adobe Photoshop and Illustrator.

## Statistical Analysis

Data from the ELISAs (ie, tau concentrations) were normalized to reduce skewness using logarithmic transformations and then used for statistical comparisons. Differences between ND, CTE stage II/III, CTE stage IV, and AD cases were determined using one-way analysis of variance tests with the Tukey post hoc analysis for all possible comparisons when overall significance was achieved. Correlations with age, disease stage, postmortem interval, and age at disease onset were performed for CTE cases using the Spearman rank correlation test. A Spearman correlation matrix was run between each tau marker in CTE cases. Significance was set at $p < 0.05$; all analyses were two-tailed. All statistical comparisons and graphs were generated using GraphPad Prism v5.0f software (GraphPad Software Inc., La Jolla, CA).

# RESULTS

## Neuronal Tau Pathology in CTE

The tau pathology labeled with TNT1, TOC1, and pS422 was irregular and focal in distribution, preferentially located around small blood vessels and very prominent at the depths of the sulci (Fig. 1; Supplementary Data 6). Immunoreactivity for PAD-exposed tau, oligomeric tau, and pS422 tau also was found in the somatodendritic compartment of many cortical neurons and neurites within the superficial cortical laminae (eg, layers II/III) (Figs. 1, 2). Notably, a number of neurons contained TNT1, TOC1, and pS422 immunoreactivity in a diffuse granular pattern (Fig. 3A, C, E), confirming that in CTE these changes in tau occur in early, pretangle pathology (50–52). With increasing pathological maturity, there is a mix of the diffuse granular staining and smaller compact inclusions (50–52); these neurons were labeled with TNT1, TOC1, and pS422 (Fig. 3B, D, F). Immunoreactivity often extended long distances from the somata in neural processes that appeared connected to the neuron (Fig. 3B, D, F). As in AD, these markers continued to label more mature NFTs (ie, intracellular NFTs), but "ghost tangles" (extracellular NFTs) were not well labeled with these markers (Fig. 2A–C). The ND cases contained little reactivity for TNT1, TOC1, or pS422 in the temporal lobe gyri (Fig. 2I–L). Immunoreactivity for TauC3 was relatively sparse and sometimes nonexistent in CTE (Figs. 1D, H, 2D).

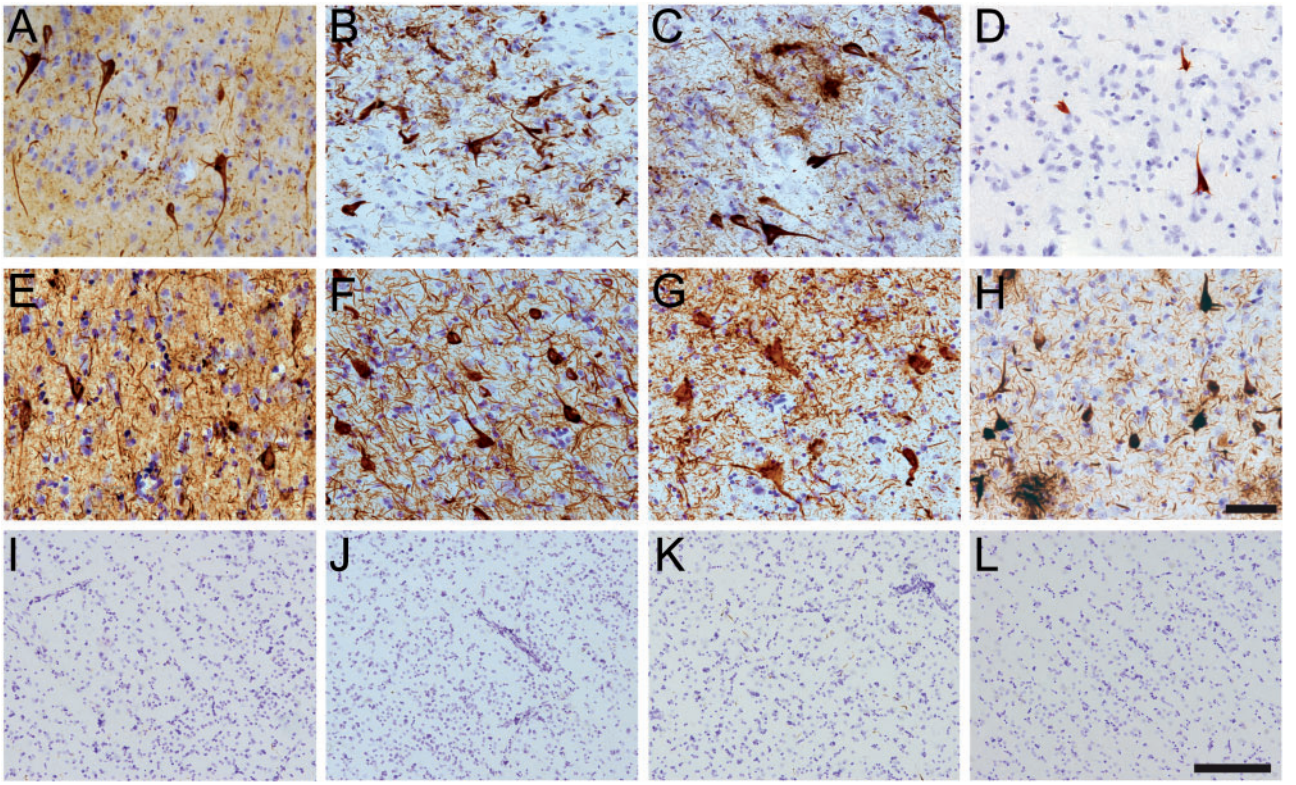


**FIGURE 2.** Neuronal tau pathology in cortical neurons in chronic traumatic encephalopathy (CTE). **(A–L)** Tissue sections from the superior frontal gyrus of CTE cases **(A–D)** and the temporal lobe of Alzheimer disease (AD) **(E–H)** and in nondemented aged control (ND) cases **(I–L)** were immunostained to characterize the gray matter pathology containing phosphatase-activating domain (PAD) exposed tau **(**TNT1-positive; **A, E, I)**, tau oligomers **(**TOC1-positive; **B, F, J)**, phospho-Ser422 tau **(**pS422-positive; **C, G, K)**, and C-terminal truncated tau **(**TauC3-positive; **D, H, L)**. Notably, the TNT1 **(A, E)**, TOC1 **(B, F)**, and pS422**(C, G)** tau pathology in CTE and AD included extensive neuropil threads and neurofibrillary tangles. In contrast, TNT1 **(I)**, TOC1 **(J)**, or pS422 **(K)** labeled very little to no pathology in the temporal lobe of ND control cases. The TauC3 marker was relatively sparse in CTE **(D)**, yet abundant in AD **(H)** and very low in ND **(L)** cases. Note that the ND images are taken at a lower magnification to show larger areas and the very low levels of immunoreactivity. Scale bar in **H**, 50 μm for **A–H**; scale bar in **L**, 200 μm for **I–L**.

ND tissue was also very rarely labeled with the TauC3 antibody (Fig. 2L). In contrast, immunoreactivity for TauC3 in AD was abundant (Fig. 2H compared to 2D and 2L), as previously established (13, 14, 16, 22). In addition to the tau pathology in the somatodendritic compartment, dystrophic axons in the white matter were labeled with TNT1, TOC1, and pS422 in CTE (Fig. 4A–C), which resembled those seen in AD with these markers (Fig. 4D–F). The colocalization between TNT1, TOC1, and pS422 was determined using triple label immunofluorescence staining. The vast majority of the pathology showed extensive colocalization for all 3 tau markers in CTE (Fig. 5A–H), but occasionally small portions of the pathology contained only single or double labeling (Fig. 5). These data indicate that PAD exposure, oligomer formation, and phosphorylation at S422 occur early and simultaneously in neurons in CTE.

## Astrocytic Tau Pathology in CTE

The glial tau pathologies in the superior frontal gyrus of CTE brains had the morphological characteristics of astrocytic tau pathologies (17, 45, 53, 54). Triple label immunofluorescence for GFAP (astrocytes), pS422 tau, and HLA-DR (microglia) was used to determine whether the glial tau pathology in CTE was within astrocytes or microglia. Confocal imaging revealed clear colocalization between GFAP and pS422 in cell bodies of astrocytes (Fig. 6A–D), and thread-like astrocytic inclusions (Fig. 6E–H); by contrast, HLA-DR and pS422 were not colocalized. Moreover, numerous dot-like structures in the neuropil, a feature commonly observed in CTE (7, 55, 56) were colabeled for GFAP and pS422, but not for HLA-DR (Fig. 6I–L).

Immunohistochemistry was used to determine whether all 3 early tau markers were present in the typical astrocytic pathologies in CTE. The TNT1, TOC1, and pS422 antibodies primarily identified clusters of astrocytes in the cortical gray matter and labeled tau inclusions in the somata and processes of astrocytes (Fig. 7), as well as occasional coiled bodies (data not shown). Robust astrocytic tau pathology was present in perivascular areas in CTE (Fig. 7D). The tau-positive astrocytes had various morphologies with prominent dot-like astrocytic immunoreactivity clustered around small blood

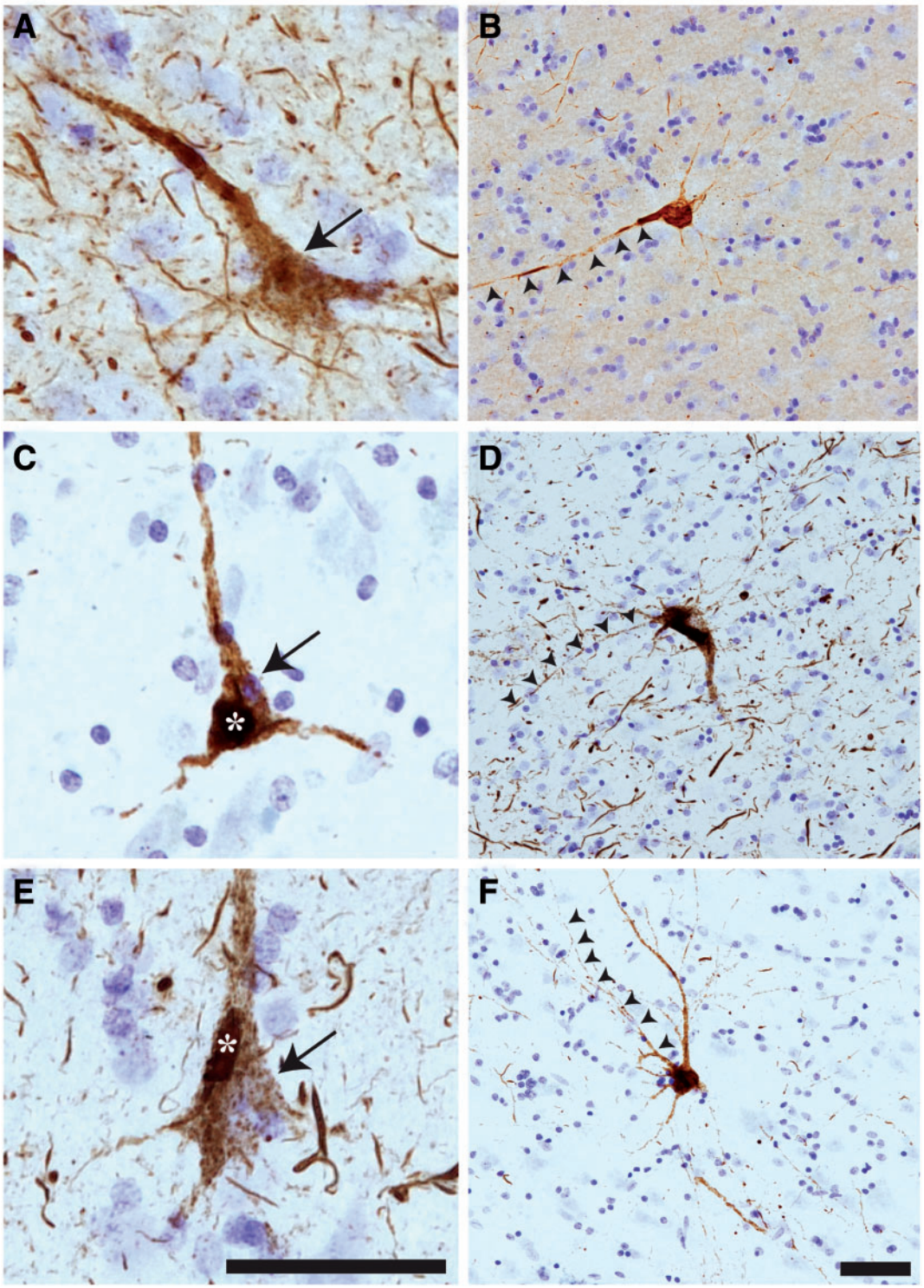


**FIGURE 3.** Early, pretangle tau pathology markers in cortical neurons in chronic traumatic encephalopathy (CTE). **(A–F)** Within the superior frontal gyrus, antibodies TNT1 **(A, B)**, TOC1 **(C, D)**, and pS422**(E, F)** all label early, pretangle pathology in pyramidal neurons that are consistent with previously described group 1 and 2 neurons (51); or stage 0/1 neurons (50, 52). The tau immunostaining in these neurons is diffuse and granular **(**arrows in **A, C, E)** with some small compact inclusions **(**asterisk in **C**, **E)**. In these early forms of tau pathology, there are often TNT1 **(B)**-, TOC1 **(D)**-, and pS422 **(F)**-immunoreactive inclusions that extend far into processes **(**arrowheads in **B, D, F)**. These patterns of staining show that TNT1, TOC1, and pS422 label early, pretangle tau pathology in CTE, and that these modifications occur early in the evolution of the tau abnormalities. Scale bar in **E**, 50 μm for **A, C, E**; scale bar in **F**, 50 μm for **B, D, F**.

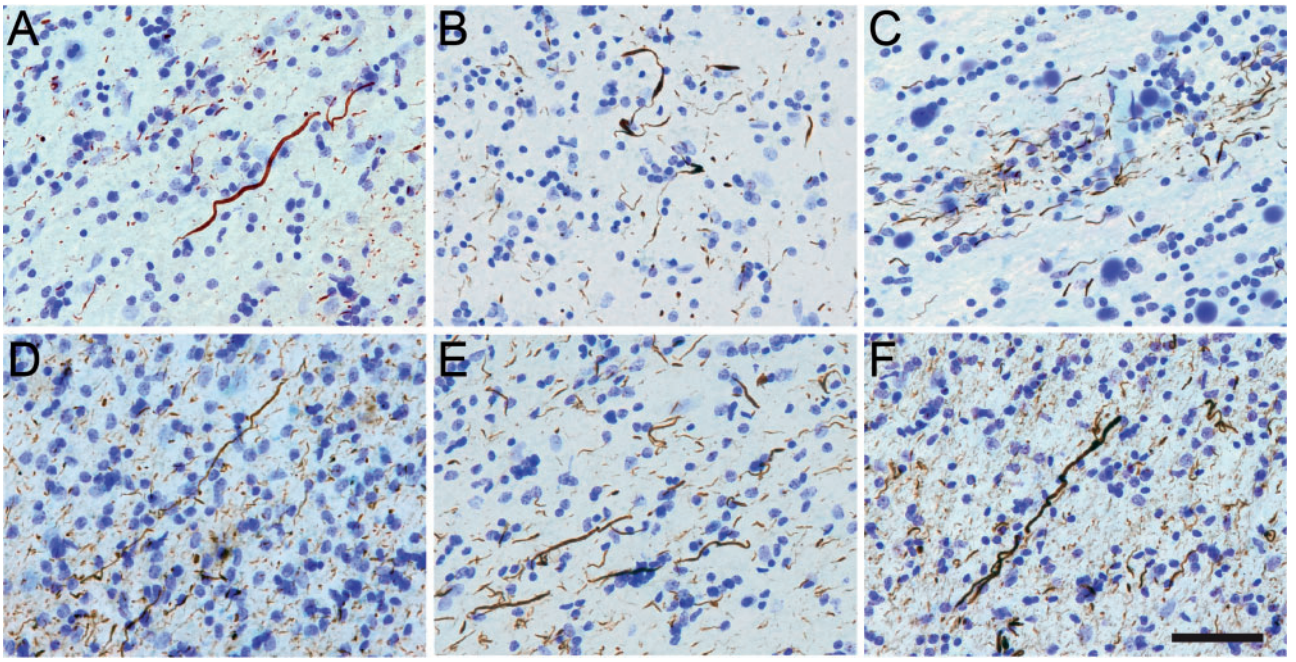


**FIGURE 4.** Axonal pathology in the white matter in chronic traumatic encephalopathy (CTE). **(A–C)** In CTE, axonal thread-like neurites were immunolabeled with TNT1 **(A)**, TOC1 **(B)**, and pS422 **(C)** antibodies. These data suggest that phosphatase-activating domain (PAD) exposure, oligomer formation, and phosphorylation of Ser422 occur in the axons in CTE. **(D–F)** Similar TNT1 **(D)**, TOC1**(E)**, and pS422 **(F)** axonal pathology was present in the white matter of Alzheimer disease (AD) brains. Scale bar in **F**, 50 μm for **A–F**.

vessels and in the neuropil (Fig. 7E-H). All astrocytic pathologies were composed of PAD-exposed, oligomeric, and phospho-S422 tau, and infrequently with TauC3, consistent with the lower levels of neuronal TauC3 pathology in CTE (Fig. 2). Colocalization of TNT1, TOC1, and pS422 in astrocytes was determined using triple label immunofluorescence staining in CTE cases. All 3 tau markers showed extensive colocalization in astrocytic somata in CTE (Fig. 8A–D). Extensive colocalization between TNT1, TOC1, and pS422 was present in the perivascular tau pathology as well as the thread (Fig. 8A–D) and dot-like structures (Fig. 8E–L). These data suggest that the appearance of PAD-exposed tau, oligomeric tau, and phosphorylated S422 tau occurs simultaneously in astrocytes of CTE brains.

## Tau Biochemistry in CTE

We used a series of sandwich ELISAs with Tau5, TNT1, TOC1, or pS422 as the capture antibody to establish the levels of these tau forms in soluble and sarkosyl insoluble fractions in the frontal cortex from ND, CTE, and AD cases. In the soluble tau fraction, all groups showed signal for total tau in the Tau5 assay, but there were no overall significant differences among the groups ($F_{3,19} = 2.855$, $p = 0.0644$; Fig. 9A). The TNT1 and TOC1 assays with soluble tau showed a progressive, significant increase in signal from ND cases (little to no signal) to CTE II/III cases and then CTE IV cases, which had similar levels to those in Braak stage VI AD samples (TNT1: $F_{3,19} = 56.54$, $p < 0.0001$; TOC1: $F_{3,19} = 88.36$, $p < 0.0001$; Fig. 9B, C). The pS422 assay of soluble tau revealed a significant increase in CTE IV cases compared to ND and CTE II/III cases, whereas AD cases had significantly higher levels than all other groups ($F_{3,19} = 45.96$, $p < 0.0001$; Fig. 9D). TauC3 signal was highest in AD cases (0.041 ng/μL) in the soluble tau fraction compared to ND (0.0036 ng/μL), CTE II/III (0.0033 ng/μL) and CTE IV (0.0056 ng/μL), which reached statistical significance compared to ND and CTE II/III cases ($F_{3,19} = 4.896$, $p = 0.011$; Fig. 9E). The ND and CTE II/III cases showed low levels of total tau in the sarkosyl insoluble tau fraction in the Tau5 assay, while strong signal was detected in CTE IV and AD cases ($F_{3,19} = 22.57$, $p < 0.0001$; Fig. 9E). Both the TNT1 and TOC1 assays of insoluble tau showed progressive, significant increases in signal from ND to CTE II/III cases and then CTE IV cases, which had similar levels to those in AD samples (TNT1: $F_{3,19} = 22.91$, $p < 0.0001$; TOC1: $F_{3,19} = 32.31$, $p < 0.0001$; Fig. 9F, G). The pS422 assay of insoluble tau revealed little reactivity in ND controls and CTE II/III cases, and a significant increase in the CTE IV cases that were similar to levels in AD cases ($F_{3,19} = 32.61$, $p < 0.0001$; Fig. 9H). Finally, the TauC3 signal in the insoluble tau fraction was highest for AD cases (0.024 ng/μL) when compared to ND (0.0034 ng/μL), CTE II/III (0.0034 ng/μL), and CTE IV (0.0048 ng/μL), which reached statistical significance compared to ND and CTE II/III cases ($F_{3,19} = 4.896$, $p = 0.011$; Fig. 9E).

Correlation analyses were used to establish the relationship between the levels of tau markers (ie, TNT1, TOC1,

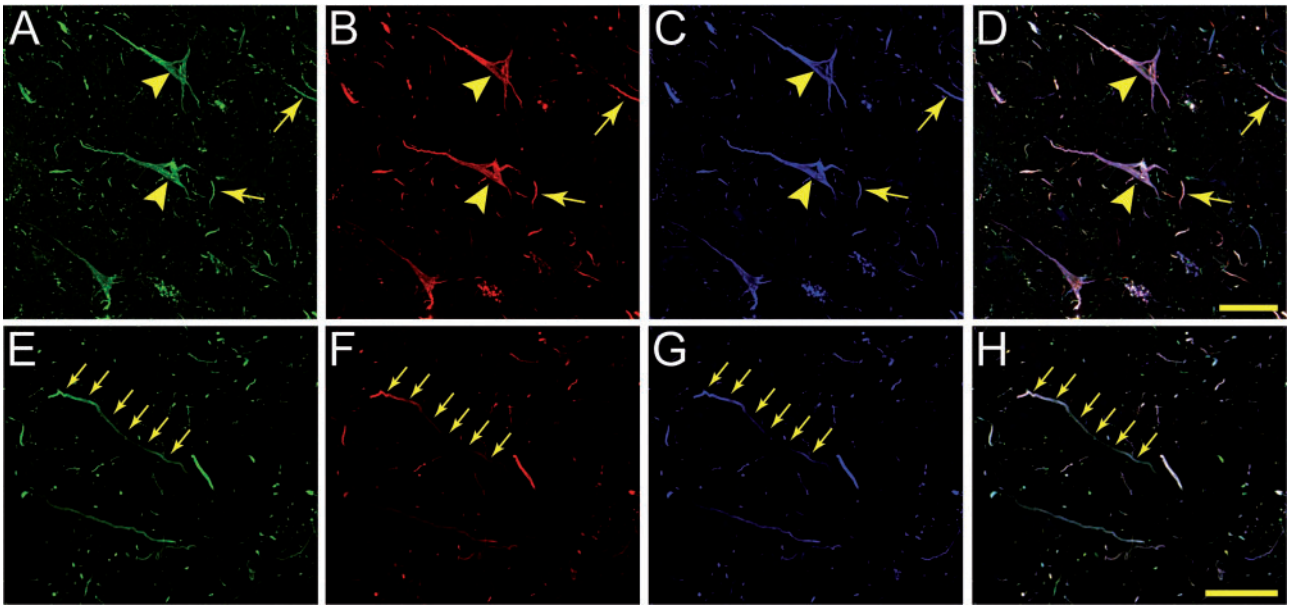


**FIGURE 5.** Colocalization of TNT1, TOC1, and pS422 tau in neuronal pathology of the chronic traumatic encephalopathy (CTE) brain. **(A–D)** Confocal microscopy was used to image multilabel immunofluorescence staining for TNT1 **(A)**, TOC1 **(B)**, and pS422 **(C)** tau markers in somatodendritic inclusions (arrowheads) and neuropil threads (arrows) in CTE **(D**, merge**)**. All 3 early, pretangle tau markers were highly colocalized in the abnormal neurons. Some discrete areas of staining contained single or double labeling indicating that these modifications can occur independently of the others. **(E–H)** The axonal pathology (arrows) in CTE white matter areas showed similar levels of colocalization between TNT1 **(E)**, TOC1 **(F)**, and pS422 **(G)** tau markers **(H**, merge**)**. Collectively, these data suggest these modified forms of tau occur at similar times during the progression of tau accumulation in CTE. Scale bars: 50 μm.

pS422, or TauC3) and either aging, disease stage, postmortem interval, or age of onset in CTE cases (Table 2). None of the tau markers used here correlated with age or age of onset, and only pS422 in the soluble fraction correlated with postmortem interval in CTE cases. Soluble total tau levels did not correlate with disease stage, but total tau levels in the insoluble fraction did correlate. TNT1, TOC1, and pS422 in both the soluble and insoluble fractions were strongly correlated with CTE stage ($p < 0.05$). The levels of TauC3 did not correlate with CTE stage in either the soluble or insoluble fractions. Finally, a correlational matrix was used to determine whether the tau markers used here are correlated with one another in CTE cases (Supplementary Data 7, correlation matrix of all tau markers). In the soluble tau fraction, TNT1, TOC1, and pS422 correlated with each other, but Tau5 and TauC3 did not correlate with other markers. Within the insoluble tau fraction the following correlations were observed: Tau5 correlated with TOC1, pS422 and TauC3; TNT1 correlated with pS422; TOC1 correlated with pS422 and TauC3; and pS422 was correlated with TauC3. The levels of TNT1, TOC1, and pS422 in the soluble fraction were correlated with the levels of the same marker in the insoluble fraction.

## DISCUSSION

Over the past several years, significant attention has focused on CTE and the pathological features of this tauopathy (10). Preliminary neuropathological diagnostic criteria for CTE were proposed in 2013 (3, 43); these were recently supported by a panel of expert neuropathologists as part of a U01 funded by the National Institute of Neurological Disorders and Stroke and National Institute of Biomedical Imaging and Bioengineering (1U01NS086659–01) (1). The majority of previous neuropathological studies have focused on common disease-relevant tau markers, such as PHF1 (pS396/pS404), AT8 (phospho-S199/S202/T205), CP13 (phospho-S202) and silver staining (6–10). In addition, prior studies suggested that CTE tau pathology is a mixture of 4-repeat and 3-repeat tau and contains additional phosphoepitopes (pT181 and pT231) (6, 12, 57). However, the involvement of PAD-exposed, oligomeric, phospho-S422, and truncated tau pathology in CTE was not known.

In the current work, we sought to identify whether some of the pathological changes in tau that characterize AD, including PAD exposure (ie, TNT1-reactive), oligomer formation (ie, TOC1-reactive), phosphorylation at serine 422 (ie, pS422-reactive), and D421 cleavage (ie, TauC3-reactive) (14, 16, 22–26), also exist in CTE. Tau pathology in CTE consists of a mixture of neuronal and astrocytic pathologies as previously noted with other tau markers (6–10). To our knowledge, this is the first demonstration that neuronal and astrocytic tau pathologies in CTE are composed of PAD-exposed, oligomeric, S422 phosphorylated tau, and D421 cleaved tau using immunohistochemical and biochemical assays. This extends previous work showing that TOC1 and pS422 colocalize in MCI and AD (25, 58) and suggests these modifications occur simultaneously during the evolution of

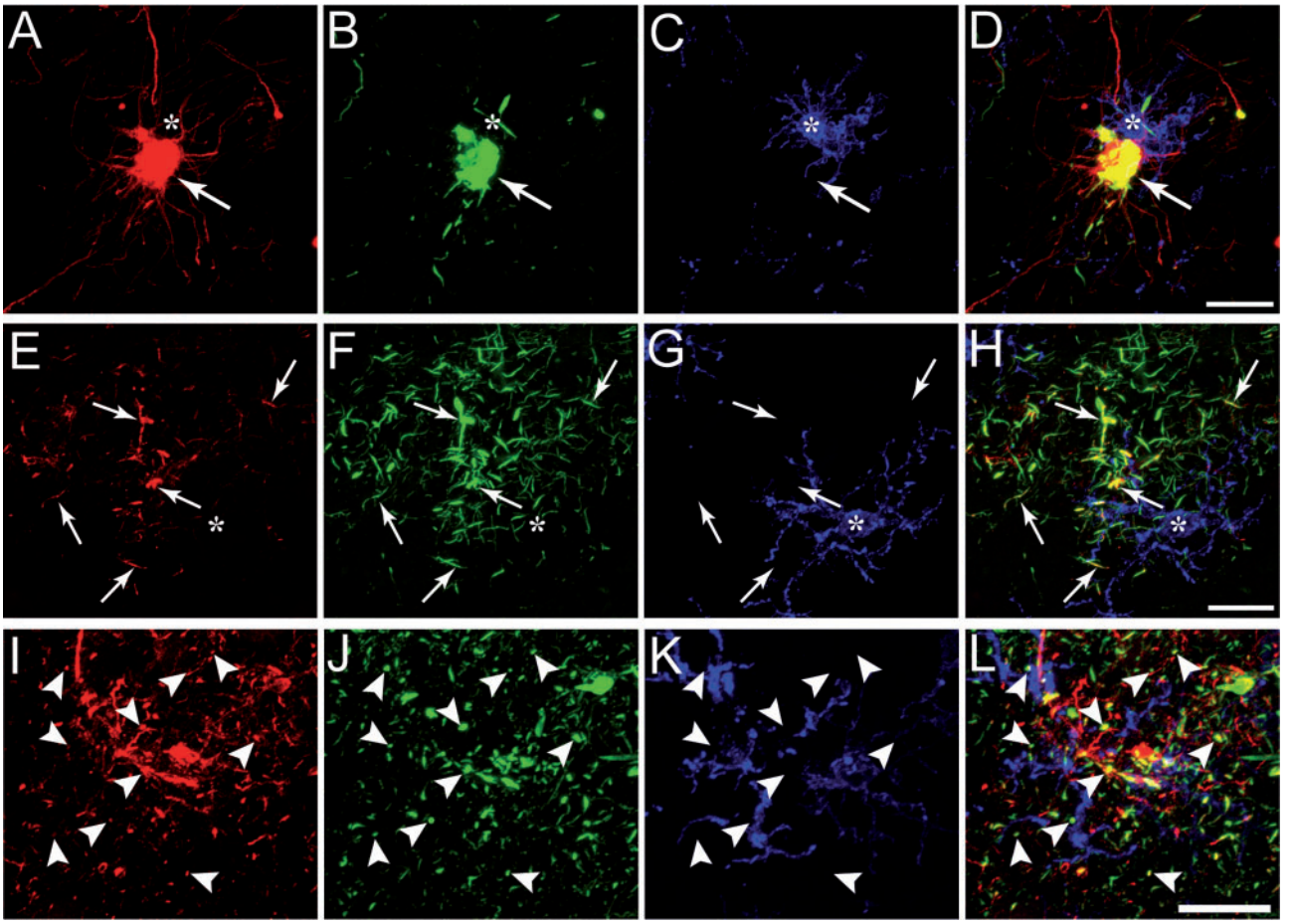


**FIGURE 6.** Glial tau pathology in astrocytes but not microglia in chronic traumatic encephalopathy (CTE). **(A–D)** The tau pathology in the somata of glial cells was confirmed to be astrocytic using triple label staining for glial fibrillary acidic protein (GFAP) for astrocytes **(A)**, pS422 tau **(B)**, and human leukocyte antigen–DR (HLA-DR, clone LN3) for microglia **(C)**. Note the colocalization**(D**, merge**)** of GFAP and pS422 tau (arrows), but lack of overlap of tau with HLA-DR (asterisk). **(E–H)** The tau pathology in glial processes was confirmed to be astrocytic using triple label staining for GFAP **(E)**, pS422 tau**(F)**, and HLA-DR**(G)**. Note the colocalization **(H**, merge**)** of GFAP and pS422 tau in thread-like structures (arrows), but lack of overlap of tau with HLA-DR (asterisk). **(I–L)** The prominent dot-like glial pathology in CTE was confirmed to be astrocytic using triple label staining for GFAP**(I)**, pS422 tau **(J)**, and HLA-DR (**K**). Note the colocalization **(L**, merge**)** of GFAP and pS422 tau (arrowheads), but not HLA-DR **(K)**. These data confirm the glial tau pathologies in CTE brains are within astrocytes, not microglia. Scale bar in **D**, 50 μm for **A–D**; scale bar in **H**, 50 μm for **E–H**; scale bar in **L**, 20 μm for **I–L**.

tau pathology in CTE. The tissue used in this study was from different tissue banks, but despite the differences in tissue origin, immunoreactivity was found with each antibody.

The earliest phase of pathological tau formation in AD is the appearance of diffuse granular inclusions in the somatodendritic compartment in neurons, referred to as "early, pretangle" neurons (50–52). The appearance of pathological epitopes in these forms of pathology is sufficient to establish them as early, pretangle tau changes. Indeed, several pathological epitopes such as AT8 (21, 24, 51, 59, 60), pS422 (15–17), TNT1 (23, 24), TOC1 (25), Alz50 (13, 14, 18, 21, 61), and pT231 (18, 21, 62) label the early diffuse granular inclusions in pretangle neurons in AD. These data are consistent with our findings in CTE, in which diffuse granular immunoreactivity for TNT1, TOC1, and pS422 appears to occur in the early phase of tau pathology. The next step in the formation of NFTs in AD is the appearance of some small compact inclusions within cells containing diffuse granular stains (50–52); again, the TNT1, TOC1, and pS422 immunoreactivity in several neurons followed this pattern in CTE. In the pretangle neurons, the tau pathology often extended long distances into the neural processes, a common feature of neurons containing early tau pathology (50–52). In AD, there is evidence of cleavage at D421 and the emergence of the TauC3 neoepitope (14, 22). The TauC3 epitope can appear early in pretangle neurons (19, 21), but appears after other earlier changes such as the Alz50 conformational change, as well as the pS422, AT8, and pT231 phosphoepitopes (13–16, 18–20). Importantly, we found that cleavage of tau at D421 does not appear to be a major event in the evolution of tau pathology in the superior frontal gyrus of CTE brains. Notably, there is a report in the literature regarding the pS422 and AT8 tau epitopes that suggests they appear later

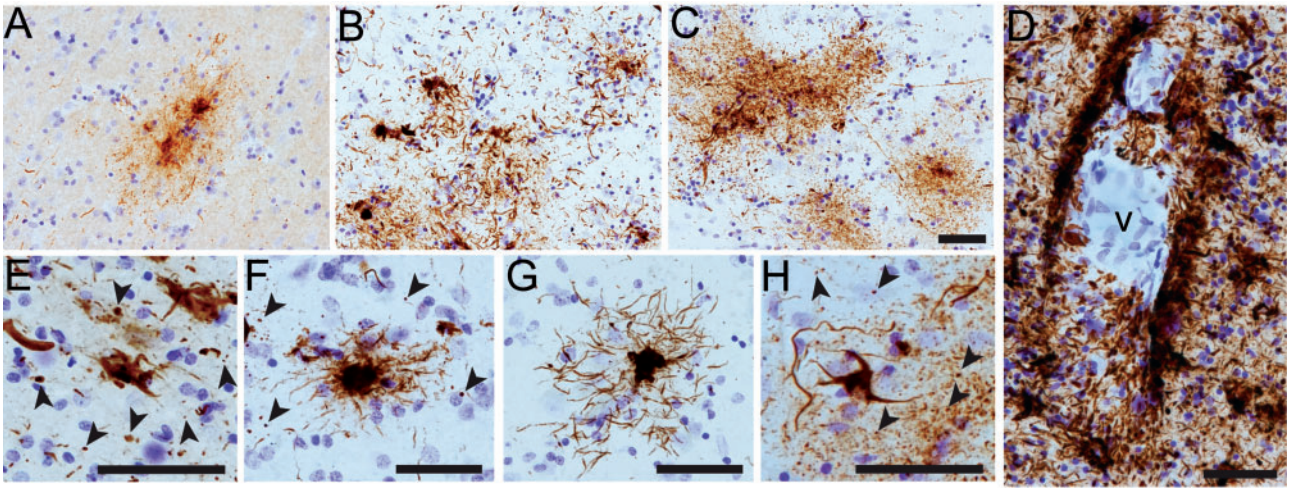


**FIGURE 7.** Astrocytic tau pathology in the superior frontal gyrus in chronic traumatic encephalopathy (CTE). **(A–C)** Clusters of tau-immunoreactive astrocytes in the gray matter immunolabeled with all 3 early tau markers: TNT1 **(A)**, TOC1 **(B)**, and pS422 **(C)**. **(D)** Extensive perivascular glial pathology was stained with all 3 markers. TOC1 is shown depicted as an illustrative example (v-vessel). **(E–H)** The somata and processes of astrocytes were extensively labeled with the TNT1 **(E)**, TOC1 **(F)** and pS422 **(G, H)** antibodies. Notably, several dot-like inclusions were labeled with all of these antibodies **(**arrowheads in **E, F, H)**. These data indicate that the typical astrocytic pathology in CTE is composed of phosphatase-activating domain (PAD)-exposed tau, oligomeric tau, and phospho-Ser422 tau. Scale bar in **C**, 50 μm for **A–C**; scale bar in **D**, 50 μm; Scale bars are 50 μm in **E–H**.

during the evolution of tau inclusion maturation in AD (63). However, several other studies clearly depict these epitopes labeling pretangle neurons, supporting their early appearance, which is consistent with the data presented here with pS422 in CTE and previously with pS422 and AT8 in AD (15–17, 21, 24, 51, 59, 60). The final step in NFT evolution is the appearance of "ghost tangles," the extracellular remains of tangle-bearing neurons (50–52). As shown in AD (15–17, 23–25), TNT1, TOC1, and pS422 continued to label more mature classic NFT tau pathology in CTE brains, but did not readily identify ghost tangles in CTE. Thus, we show that TNT1, TOC1, and pS422 appear as early, pretangle changes in CTE and their presence is continued as NFTs continue to mature, which is consistent with most previous reports describing their appearance in AD.

We also showed that the primary glial pathology in CTE is in astrocytes not microglia. For these experiments, we used the pS422 marker as a representative stain because all 3 early tau markers were highly colocalized and because it is a rabbit antibody, pS422 is compatible with the anti-GFAP and anti-HLA-DR mouse antibodies for triple staining. Several morphologies of astrocytes containing tau pathology were observed with an abundance of dot-like structures in CTE (7, 55, 56), which were especially prominent in perivascular are as. The presence of robust astrocyte pathology suggests there may be overlapping mechanisms to other non-AD tauopathies that primarily involve astrocytic inclusions, such as progressive supranuclear palsy and corticobasal degeneration (54). The repeated, mild head injuries that cause CTE may disrupt the blood-brain-barrier and facilitate inflammation and/or glial abnormalities that contribute to formation of glial tau inclusions, as well as the perivascular neuronal pathologies. Interestingly, microglia were not labeled with these tau markers, suggesting that microglia-associated phagocytosis of extracellular tau or endogenous microglial tau are not the source of glial inclusions in CTE.

We confirmed the immunohistochemical findings by identifying the presence of PAD-exposed tau, oligomeric tau, pS422 tau, and C-terminal truncated tau biochemically in CTE and compared the findings to ND and AD. Only one previous study detailed the biochemical characteristics of tau in CTE (12) other than analysis of total tau levels (11). Schmidt et al demonstrated that tau isolated from 2 CTE (dementia pugilistica) cases contained all 6 tau isoforms, as well as phospho-serine 396 (T3P antibody) and phospho-threonine 231 (PHF6 antibody) tau species (12). In this study, we found that important conformation changes in tau (eg, PAD-exposed tau, oligomeric tau) and an early phosphoepitope (pS422), occur in CTE, and that these markers were well correlated with CTE staging. The TauC3 ELISA confirmed the IHC results showing little TauC3 in CTE (and ND) cases, and TauC3 did not correlate with CTE stage. The extensive colocalization between TNT1, TOC1, and pS422 was further confirmed using a correlational matrix comparison because all of these markers were strongly correlated with one another in the soluble fraction and insoluble fraction, (except insoluble TNT1 and TOC1). Interestingly, TNT1, TOC1, and pS422 did not correlate with Tau5 or TauC3 in the soluble fraction suggesting the level of these forms of tau are not driven by total tau levels or related to C-terminal truncation in soluble tau. The amounts of TNT1, TOC1, or pS422 in the soluble and insoluble fractions were well correlated, suggesting the presence of these modifications is linked between these 2 pools of tau species. Collectively, these data support a close relationship between PAD exposure, oligomer formation, and phosphorylation at S422 in CTE.

A notable dissimilarity between CTE and ND cases was identified in the IHC and biochemical assays for TNT1,

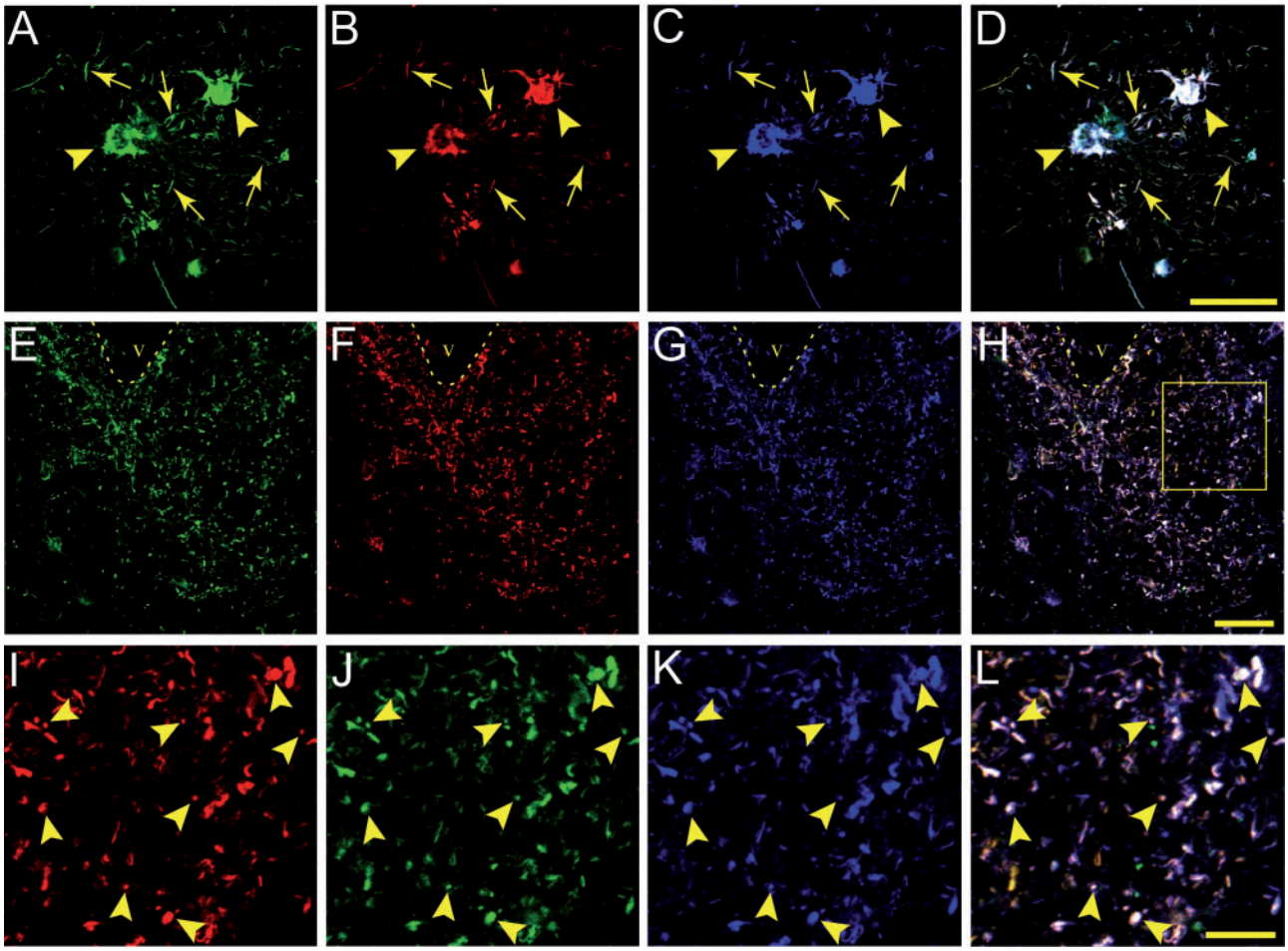


**FIGURE 8.** Colocalization of TNT1 tau, TOC1 tau, and pS422 tau in astrocytes in chronic traumatic encephalopathy (CTE). **(A–D)** Astrocytic tau pathology in the superior frontal gyrus area stained with TNT1 **(A)**, TOC1 **(B)**, and pS422 **(C)** antibodies; merged image is shown in **(D)**. Note that all 3 early tau markers colocalize in the somata (arrowheads) and processes (arrows) of astrocytes. **(E–H)** TNT1 **(E)**, TOC1 **(F)**, and pS422 **(G)** are extensively colocalized**(H**, merge**)** in the perivascular tau pathology in CTE (v-vessel). **(I–L)** High magnification of dot-like pathology in boxed area from **(H)** labeled with TNT1 **(I)**, TOC1 **(J)**, pS422 **(K)** antibodies. The merged image **(L)** shows the colocalization of all 3 early tau markers in the astrocytic dot-like perivascular pathology in CTE (arrowheads). These data demonstrate that phosphatase-activating domain exposed, oligomeric, and phospho-S422 tau coexist simultaneously in astrocytic pathology in CTE. Scale bar in **D**, 50 μm for **A–D**; scale bar in **H**, 50 μm for **E–H**; scale bar in **L**, 20 μm for **I–L**.

TOC1, or pS422. In the temporal cortex of ND cases, TNT1, TOC1, pS422, and TauC3-immunoreactive pathology was exceptionally sparse. The temporal cortex of ND cases was used primarily because this is an aging-vulnerable region of the brain for developing tau pathology. Thus, it is unlikely that the use of temporal lobe for ND and frontal cortex for CTE is responsible for the contrast between these cases. Our conclusion that these pathological forms of tau are present in CTE, but not ND cases, is further supported by the biochemical analyses of both the soluble and sarkosyl insoluble tau fractions from the frontal cortex of ND, CTE, and AD cases. The CTE II/III and CTE IV cases were positive for TNT1 or TOC1, which contrasted with little to no reactivity in the same brain region of ND controls. Interestingly, in this small sample set, none of the tau markers was correlated with age or age of onset among the CTE cases, suggesting that the CTE pathology is not driven primarily by age-related variables. Moreover, CTE IV cases had high levels of pS422 tau, while ND cases did not. These data support a clear distinction between CTE and normal age-related tau deposition. These assays also highlight biochemical similarities in some tau species in late-stage CTE (stage IV) and late-stage AD (Braak V–VI).

The finding of TNT1, TOC1, and pS422 positive inclusions has important implications for the pathogenesis of tau pathology in CTE. Recently, we showed that PAD exposure is a mechanism by which tau can directly impair anterograde fast axonal transport (23, 24, 27), which could contribute to axonal dysfunction and eventually neurodegeneration (31, 64). Axonal dysfunction is a prominent feature of traumatic

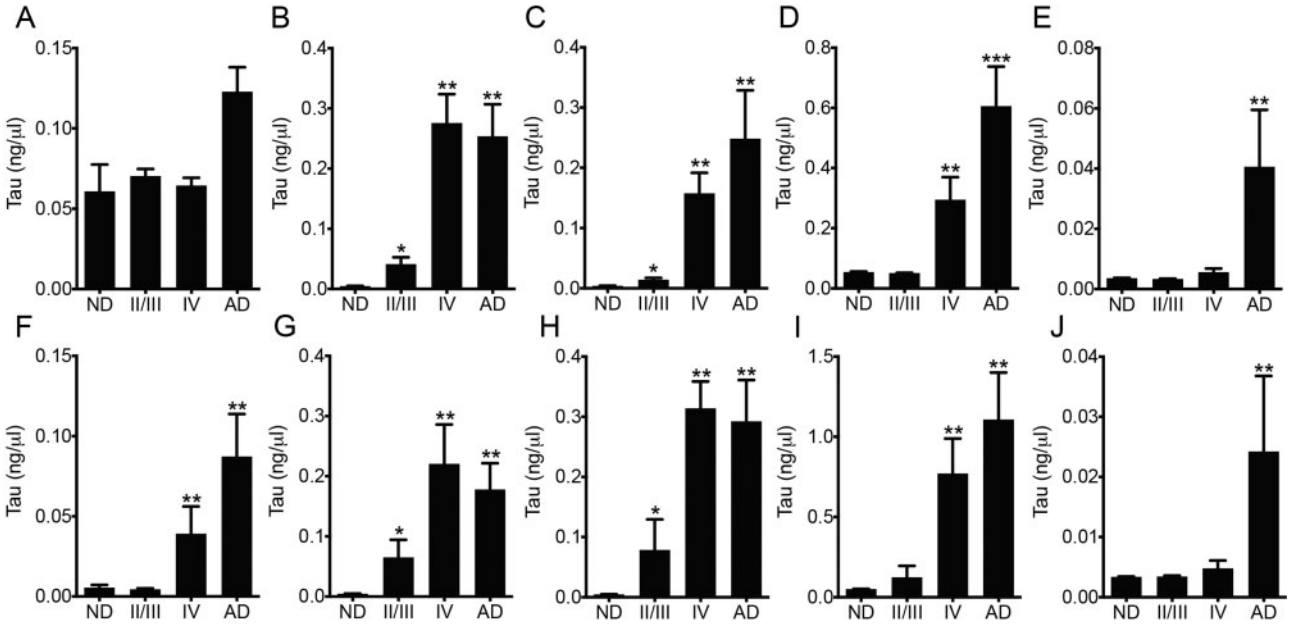


**FIGURE 9.** Biochemical analysis of total tau, phosphatase-activating domain (PAD) exposed tau, oligomeric tau, phospho-S422 tau, and tau truncated at the C-terminus in soluble tau and sarkosyl insoluble tau fractions from the frontal cortex of nondemented controls (ND), chronic traumatic encephalopathy (CTE), and Alzheimer disease (AD) patient brains. **(A–E)** Sandwich ELISAs were used to quantify soluble tau fractions for total tau (Tau5 capture) **(A)**, PAD-exposed tau (TNT1 capture) **(B)**, tau oligomers (TOC1 capture) **(C)**, pS422 tau (pS422 capture) **(D)**, and C-terminal truncated tau (TauC3 capture) **(E)**. As expected, the soluble fraction contained substantial tau proteins in all groups **(A)**, overall significance was not reached between groups ($p = 0.0644$). Both TNT1- and TOC1-reactive tau species are progressively increased in CTE II/III and then CTE IV subjects, the latter of which were similar to the values in the AD cases. pS422 tau was undetectable/very low in ND and CTE II/III cases **(D)**, but significantly increased in CTE IV and further increased in AD cases. AD cases contained the highest levels of TauC3 (~8 times the amount in ND, CTE II/III, and IV cases), which reached statistical significance compared to ND and CTE II/III cases **(E)**. **(F–J)** Sandwich ELISAs of sarkosyl insoluble tau fractions for total tau **(F)**, PAD-exposed tau **(G)**, tau oligomers **(H)**, pS422 tau **(I)**, and TauC3 **(J)** showed similar results as soluble tau, with the exceptions that total tau was significantly elevated in CTE IV and AD cases compared to ND and CTE II/III cases; similar levels of pS422 were present in CTE IV and AD cases. These data suggest that PAD-exposed and oligomeric tau progressively accumulates in CTE, pS422 is robustly increased in CTE IV, and that CTE cases have very low levels of TauC3, similar to ND cases. *$p < 0.05$ vs ND; **$p < 0.05$ vs ND and CTE II/III; ***$p < 0.05$ vs ND, CTE II/III, and CTE IV.

**TABLE 2.** Spearman Correlation Analysis of Tau Levels Vs Age, Disease Stage, Postmortem Interval, or Age at Disease Onset in Chronic Traumatic Encephalopathy Cases

| | Tau5 Sol | Tau5 Insol | TNT1 Sol | TNT1 Insol | TOC1 Sol | TOC1 Insol | pS422 Sol | pS422 Insol | TauC3 Sol | TauC3 Insol |
|---|---|---|---|---|---|---|---|---|---|---|
| Age vs | $0.009^{ns}$ | $0.418^{ns}$ | $0.564^{ns}$ | $0.300^{ns}$ | $0.527^{ns}$ | $0.502^{ns}$ | $0.365^{ns}$ | $0.309^{ns}$ | $-0.330^{ns}$ | $0.069^{ns}$ |
| Stage vs | $-0.297^{ns}$ | 0.829** | 0.854** | 0.628* | 0.854** | 0.757* | 0.869** | 0.809** | $0.213^{ns}$ | $0.552^{ns}$ |
| PMI vs | $0.436^{ns}$ | $0.383^{ns}$ | $0.441^{ns}$ | $0.043^{ns}$ | $0.446^{ns}$ | $0.378^{ns}$ | 0.615* | $0.441^{ns}$ | $0.039^{ns}$ | $0.484^{ns}$ |
| Onset vs | $-0.358^{ns}$ | $0.539^{ns}$ | $0.588^{ns}$ | $0.321^{ns}$ | $0.527^{ns}$ | $0.457^{ns}$ | $0.552^{ns}$ | $0.309^{ns}$ | $0.055^{ns}$ | $0.189^{ns}$ |

r values are displayed; Insol, sarkosyl insoluble tau fraction; ns, not significant; PMI, postmortem interval; pS422, phospho S422; Sol., soluble tau fraction; TauC3, cleaved at D421; Tau5, pan-tau; TOC1, oligomeric tau; TNT1, phosphatase-activating domain (PAD) tau.

*$p \leq 0.05$.

**$p \leq 0.01$.

brain injury-related pathology and several lines of evidence from animal models, culture models, and human traumatic brain injury cases support a primary role for axonal dysfunction in posttraumatic neurodegeneration (65–68). In this study, we identified PAD-exposed tau, oligomeric tau, and phospho-S422 tau in the axonal pathologies of CTE. Notably, disease-related modifications, such as oligomer formation, are the mechanisms by which PAD becomes aberrantly exposed, suggesting that oligomeric tau is potentially neurotoxic through PAD-mediated pathways that disrupt axonal function in CTE.

AT8 also labels early pretangle neurons in CTE (6) (as well as AD, [21, 24, 51, 60, 61]), and AT8 was recently identified as a modification that exposes PAD and disrupts axonal transport (24, 69). Moreover, the toxicity of tau oligomers is currently a target of active investigation by many groups, and several studies using both animal and cell culture models support tau oligomers as a toxic form of tau (29, 34, 36, 37, 70, 71). A recent report found tau oligomers in a fluid percussion model of traumatic brain injury in mice (72), and now we provide human tissue-based evidence that tau oligomers are present in CTE brains. Finally, the progressive deposition of pS422 reactive tau pathology in the cholinergic basal forebrain correlates well with progressive cognitive decline from ND to MCI and then AD (15). This suggests that pS422 is associated with neuronal dysfunction and cognitive decline in AD, and may also be related to cognitive decline or other functional impairments in individuals with CTE. Thus, the tau pathology in CTE brains also exists in forms that are likely contributing to axonal dysfunction, neurodegeneration, and cognitive decline in patients with CTE.

In summary, we demonstrate PAD exposure, oligomer formation, and phosphorylation of S422 in the distinctive neuronal and astrocytic tau pathologies that characterize CTE using qualitative IHC and quantitative biochemistry. The work presented here further supports accumulating data demonstrating that CTE is a distinctive tauopathy that can be distinguished from AD and age-related tauopathy not only by the nature and distribution of the pathology, but by immunohistochemical and biochemical analyses. Previous work has established that both 4R and 3R isoforms of tau are found in CTE; more detailed biochemical characterization of isoform composition within TNT1, TOC1, and pS422 pathologies in CTE will be required to understand the contribution of each isoform to early tau pathology. Future studies identifying additional posttranslational modifications and the chronological ordering of various forms of tau in several brain regions during CTE progression may provide important insights into mechanisms of CTE pathogenesis after traumatic injury and potential targets for tau-based therapeutic interventions. Similarly, the phosphoepitopes that coexist with PAD-exposed and/or oligomeric tau may provide further insight into the posttranslational modifications that facilitate conformational changes in CTE that might contribute to pathogenesis. Finally, studies that correlate the progression of tau pathological changes to clinical outcome measures will help determine the contribution of tau abnormalities to the clinical manifestations of CTE.

## ACKNOWLEDGMENTS

*We would like to dedicate this work to the late Lester "Skip" Binder. His substantial and instrumental contributions to the field of tau biology were critical to this work and will continue to advance our understanding of tauopathies for many years to come. We gratefully acknowledge the use of resources and facilities at the Edith Nourse Rogers Memorial Veterans Hospital (Bedford, MA). We also gratefully acknowledge the help of all members of the CTE Program at Boston University and the Boston VA, and the individuals and families whose participation and contributions made this work possible. We are grateful to Dr. Thomas Beach and the Banner Sun Health Research Institute Brain and Body Donation Program of Sun City, Arizona for the provision of human biological materials (ie, brain tissue sections). We gratefully acknowledge the assistance of this Neuropathology Core in the Alzheimer Disease Core Center at Northwestern University, Chicago, IL.*

## REFERENCES

1. Kiernan PT, Montenigro PH, Solomon TM, et al. Chronic traumatic encephalopathy: A neurodegenerative consequence of repetitive traumatic brain injury. Sem Neurol 2015;35:20–8
2. Ling H, Hardy J, Zetterberg H. Neurological consequences of traumatic brain injuries in sports. Molec Cell Neurosci 2015;66:114–22
3. McKee AC, Daneshvar DH. The neuropathology of traumatic brain injury. Handb Clin Neurol 2015;127:45–66
4. Martland HS. Punch drunk. JAMA 1928:91;1103–7
5. Corsellis JA, Bruton CJ, Freeman-Browne D. The aftermath of boxing. Psychol Med 1973;3:270–303
6. Geddes JF, Vowles GH, Nicoll JA, et al. Neuronal cytoskeletal changes are an early consequence of repetitive head injury. Acta Neuropathol 1999;98:171–8
7. McKee AC, Stern RA, Nowinski CJ, et al. The spectrum of disease in chronic traumatic encephalopathy. Brain 2013;136:43–64
8. Ikonomovic MD, Uryu K, Abrahamson EE, et al. Alzheimer's pathology in human temporal cortex surgically excised after severe brain injury. Exp Neurol 2004;190:192–203
9. Goldstein LE, Fisher AM, Tagge CA, et al. Chronic traumatic encephalopathy in blast-exposed military veterans and a blast neurotrauma mouse model. Science Transl Med 2012;4:134ra60
10. McKee AC, Cantu RC, Nowinski CJ, et al. Chronic traumatic encephalopathy in athletes: progressive tauopathy after repetitive head injury. J Neuropathol Exp Neurol 2009;68:709–35
11. Kokjohn TA, Maarouf CL, Daugs ID, et al. Neurochemical profile of dementia pugilistica. J Neurotrauma 2013;30:981–97
12. Schmidt ML, Zhukareva V, Newell KL, et al. Tau isoform profile and phosphorylation state in dementia pugilistica recapitulate Alzheimer's disease. Acta Neuropathol 2001;101:518–24
13. Binder LI, Guillozet-Bongaarts AL, Garcia-Sierra F, et al. Tau, tangles, and Alzheimer's disease. Biochim Biophys Acta 2005;1739:216–23
14. Guillozet-Bongaarts AL, Garcia-Sierra F, et al. Tau truncation during neurofibrillary tangle evolution in Alzheimer's disease. Neurobiol Aging 2005;26:1015–22
15. Vana L, Kanaan NM, Ugwu IC, et al. Progression of tau pathology in cholinergic Basal forebrain neurons in mild cognitive impairment and Alzheimer's disease. Am J Pathol 2011;179:2533–50
16. Guillozet-Bongaarts AL, Cahill ME, Cryns VL, et al. Pseudophosphorylation of tau at serine 422 inhibits caspase cleavage: in vitro evidence and implications for tangle formation in vivo. J Neurochem 2006;97:1005–14
17. Guillozet-Bongaarts AL, Glajch KE, Libson EG, et al. Phosphorylation and cleavage of tau in non-AD tauopathies. Acta Neuropathol 2007;113:513–20
18. Flores-Rodriguez P, Ontiveros-Torres MA, Cardenas-Aguayo MC, et al. The relationship between truncation and phosphorylation at the C-terminus of tau protein in the paired helical filaments of Alzheimer's disease. Front Neurosci 2015;9:33
19. Rissman RA, Poon WW, Blurton-Jones M, et al. Caspase-cleavage of tau is an early event in Alzheimer disease tangle pathology. J Clin Invest 2004;114:121–30
20. Mondragon-Rodriguez S, Basurto-Islas G, Santa-Maria I, et al. Cleavage and conformational changes of tau protein follow phosphorylation during Alzheimer's disease. Int J Exp Pathol 2008;89:81–90
21. Luna-Munoz J, Chavez-Macias L, Garcia-Sierra F, et al. Earliest stages of tau conformational changes are related to the appearance of a sequence of specific phospho-dependent tau epitopes in Alzheimer's disease. J Alzheimer's Dis 2007;12:365–75

22. Gamblin TC, Chen F, Zambrano A, et al. Caspase cleavage of tau: Linking amyloid and neurofibrillary tangles in Alzheimer's disease. Proc Natl Acad Sci USA 2003;100:10032–7
23. Kanaan NM, Morfini G, Pigino G, et al. Phosphorylation in the amino terminus of tau prevents inhibition of anterograde axonal transport. Neurobiol Aging 2012;33:826.e15–30
24. Kanaan NM, Morfini GA, LaPointe NE, et al. Pathogenic forms of tau inhibit kinesin-dependent axonal transport through a mechanism involving activation of axonal phosphotransferases. J Neurosci 2011; 31:9858–68
25. Patterson KR, Remmers C, Fu Y, et al. Characterization of prefibrillar Tau oligomers in vitro and in Alzheimer disease. J Biol Chem 2011;286: 23063–76
26. Ward SM, Himmelstein DS, Lancia JK, et al. TOC1: Characterization of a selective oligomeric tau antibody. J Alzheimer's Dis 2013;37: 593–602
27. LaPointe NE, Morfini G, Pigino G, et al. The amino terminus of tau inhibits kinesin-dependent axonal transport: Implications for filament toxicity. J Neurosci Res 2009;87:440–51
28. Patterson KR, Ward SM, Combs B, et al. Heat shock protein 70 prevents both tau aggregation and the inhibitory effects of preexisting tau aggregates on fast axonal transport. Biochemistry 2011;50:10300–10
29. Ward SM, Himmelstein DS, Lancia JK, et al. Tau oligomers and tau toxicity in neurodegenerative disease. Biochem Soc Trans 2012;40: 667–71
30. Ward SM, Himmelstein DS, Ren Y, et al. TOC1: a valuable tool in assessing disease progression in the rTg4510 mouse model of tauopathy. Neurobiol Dis 2014;67:37–48
31. Kanaan NM, Pigino GF, Brady ST, et al. Axonal degeneration in Alzheimer's disease: when signaling abnormalities meet the axonal transport system. Exp Neurol 2013;246:44–53
32. Kuchibhotla KV, Wegmann S, Kopeikina KJ, et al. Neurofibrillary tangle-bearing neurons are functionally integrated in cortical circuits in vivo. Proc Natl Acad Sci USA 2014;111:510–4
33. Morsch R, Simon W, Coleman PD. Neurons may live for decades with neurofibrillary tangles. J Neuropathol Exp Neurol 1999;58:188–97
34. Sahara N, Ren Y, Ward S, et al. Tau oligomers as potential targets for early diagnosis of tauopathy. J Alzheimer's Dis 2014;40 Suppl 1:S91–6
35. Gadad BS, Britton GB, Rao KS. Targeting oligomers in neurodegenerative disorders: Lessons from α-synuclein, tau, and amyloid-β peptide. J Alzheimer's Dis 2011;24 Suppl 2:223–32
36. Lasagna-Reeves CA, Castillo-Carranza DL, Jackson GR, et al. Tau oligomers as potential targets for immunotherapy for Alzheimer's disease and tauopathies. Curr Alz Res 2011;8:659–65
37. Guzman-Martinez L, Farias GA, Maccioni RB. Tau oligomers as potential targets for Alzheimer's diagnosis and novel drugs. Front Neurol 2013;4:167
38. Castillo-Carranza DL, Gerson JE, Sengupta U, et al. Specific targeting of tau oligomers in Htau mice prevents cognitive impairment and tau toxicity following injection with brain-derived tau oligomeric seeds. J Alzheimer's Dis 2014;40 Suppl 1:S97–s111
39. Tian H, Davidowitz E, Lopez P, et al. Trimeric tau is toxic to human neuronal cells at low nanomolar concentrations. Int J Cell Biol 2013;2013:260787
40. Lasagna-Reeves CA, Castillo-Carranza DL, Guerrero-Muoz MJ, et al. Preparation and characterization of neurotoxic tau oligomers. Biochemistry 2010;49:10039–41
41. Chung CW, Song YH, Kim IK, et al. Proapoptotic effects of tau cleavage product generated by caspase-3. Neurobiol Dis 2001;8:162–72
42. Fasulo L, Ugolini G, Visintin M, et al. The neuronal microtubule-associated protein tau is a substrate for caspase-3 and an effector of apoptosis. J Neurochem 2000;75:624–33
43. McKee AC, Daneshvar DH, Alvarez VE, et al. The neuropathology of sport. Acta Neuropathol 2014;127:29–51
44. Beach TG, Adler CH, Sue LI, et al. Arizona Study of Aging and Neurodegenerative Disorders and Brain and Body Donation Program. Neuropathology 2015;35:354–89
45. Berry RW, Sweet AP, Clark FA, et al. Tau epitope display in progressive supranuclear palsy and corticobasal degeneration. J Neurocytol 2004;33: 287–95
46. Carmel G, Mager EM, Binder LI, et al. The structural basis of monoclonal antibody Alz50's selectivity for Alzheimer's disease pathology. J Biol Chem 1996;271:32789–95
47. Kanaan NM, Kordower JH, Collier TJ. Age-related accumulation of Marinesco bodies and lipofuscin in rhesus monkey midbrain dopamine neurons: Relevance to selective neuronal vulnerability. J Comp Neurol 2007;502:683–700
48. Kanaan NM, Kordower JH, Collier TJ. Age-related changes in glial cells of dopamine midbrain subregions in rhesus monkeys. Neurobiol Aging 2010;31:937–52
49. Kanaan NM, Kordower JH, Collier TJ. Age and region-specific responses of microglia, but not astrocytes, suggest a role in selective vulnerability of dopamine neurons after 1-methyl-4-phenyl-1,2,3,6-tetrahydropyridine exposure in monkeys. Glia 2008;56:1199–214
50. Bancher C, Brunner C, Lassmann H, et al. Tau and ubiquitin immunoreactivity at different stages of formation of Alzheimer neurofibrillary tangles. Prog Clin Biol Res 1989;317:837–48
51. Braak E, Braak H, Mandelkow EM. A sequence of cytoskeleton changes related to the formation of neurofibrillary tangles and neuropil threads. Acta Neuropathol 1994;87:554–67
52. Duong T, Doucette T, Zidenberg NA, et al. Microtubule-associated proteins tau and amyloid P component in Alzheimer's disease. Brain Res 1993;603:74–86
53. Berry RW, Quinn B, Johnson N, et al. Pathological glial tau accumulations in neurodegenerative disease: Review and case report. Neurochem Internat 2001;39:469–79
54. Dickson DW. Neuropathologic differentiation of progressive supranuclear palsy and corticobasal degeneration. J Neurol 1999;246 Suppl 2:Ii6–15
55. Hof PR, Bouras C, Buee L, et al. Differential distribution of neurofibrillary tangles in the cerebral cortex of dementia pugilistica and Alzheimer's disease cases. Acta Neuropathol 1992;85:23–30
56. Tokuda T, Ikeda S, Yanagisawa N, et al. Re-examination of ex-boxers' brains using immunohistochemistry with antibodies to amyloid beta-protein and tau protein. Acta Neuropathol 1991;82:280–5
57. Ling H, Kara E, Revesz T, et al. Concomitant progressive supranuclear palsy and chronic traumatic encephalopathy in a boxer. Acta Neuropathologica Comm 2014;2:24
58. Mufson EJ, Ward S, Binder L. Prefibrillar tau oligomers in mild cognitive impairment and Alzheimer's disease. Neurodegen Dis 2014;13:151–3
59. Garcia-Sierra F, Hauw JJ, Duyckaerts C, et al. The extent of neurofibrillary pathology in perforant pathway neurons is the key determinant of dementia in the very old. Acta Neuropathol 2000;100:29–35
60. Mondragon-Rodriguez S, Perry G, Luna-Munoz J, et al. Phosphorylation of tau protein at sites Ser(396-404) is one of the earliest events in Alzheimer's disease and Down syndrome. Neuropathol Appl Neurobiol 2014;40:121–35
61. Garcia-Sierra F, Ghoshal N, Quinn B, et al. Conformational changes and truncation of tau protein during tangle evolution in Alzheimer's disease. J Alzheimer's Dis 2003;5:65–77
62. Luna-Munoz J, Garcia-Sierra F, Falcon V, et al. Regional conformational change involving phosphorylation of tau protein at the Thr231, precedes the structural change detected by Alz-50 antibody in Alzheimer's disease. J Alzheimer's Dis 2005;8:29–41
63. Augustinack JC, Schneider A, Mandelkow EM, et al. Specific tau phosphorylation sites correlate with severity of neuronal cytopathology in Alzheimer's disease. Acta Neuropathol 2002;103:26–35
64. Morfini GA, Burns M, Binder LI, et al. Axonal transport defects in neurodegenerative diseases. J Neurosci 2009;29:12776–86
65. Blennow K, Hardy J, Zetterberg H. The neuropathology and neurobiology of traumatic brain injury. Neuron 2012;76:886–99
66. Mez J, Stern RA, McKee AC. Chronic traumatic encephalopathy: Where are we and where are we going? Curr Neurol Neurosci Rep 2013;13:407
67. Johnson VE, Stewart W, Smith DH. Axonal pathology in traumatic brain injury. Exp Neurol 2013;246:35–43
68. Siedler DG, Chuah MI, Kirkcaldie MT, et al. Diffuse axonal injury in brain trauma: Insights from alterations in neurofilaments. Front Cell Neurosci 2014;8:429
69. Jeganathan S, Hascher A, Chinnathambi S, et al. Proline-directed pseudo-phosphorylation at AT8 and PHF1 epitopes induces a compaction of the paperclip folding of tau and generates a pathological (MC-1) conformation. J Biol Chem 2008;283:32066–76

70. Cardenas-Aguayo Mdel C, Gomez-Virgilio L, DeRosa S, et al. The role of tau oligomers in the onset of Alzheimer's disease neuropathology. ACS Chem Neurosci 2014;5:1178–91
71. Sahara N, Maeda S, Takashima A. Tau oligomerization: A role for tau aggregation intermediates linked to neurodegeneration. Curr Alzheimer Res 2008;5:591–8
72. Hawkins BE, Krishnamurthy S, Castillo-Carranza DL, et al. Rapid accumulation of endogenous tau oligomers in a rat model of traumatic brain injury: Possible link between traumatic brain injury and sporadic tauopathies. J Biol Chem 2013;288:17042–50